

Optimum design of normal and high strength SFRCs: limit states and performance classes

M.Yalcin, C. Tasdemir & M.A. Tasdemir

Istanbul Technical University, Department of Civil Engineering, Istanbul, Turkey

I. Gokalp

Akansa Cement Industry and Trading Co., Betonsa Technological Center, Istanbul, Turkey

M. Yerlikaya

Bekaert Co., Kocaeli, Turkey

ABSTRACT: For determining the performance classes of steel fiber reinforced concretes (SFRCs), their equivalent flexural strength values were investigated according to both Serviceability Limit State and Ultimate Limit State. For a certain concrete class, the equivalent flexural tensile strengths depend on both the fiber volume fraction and the fiber aspect ratio. The mixtures with the longer steel fibers provide higher equivalent flexural tensile strength values than those of shorter ones. Performance classification of SFRCs can be made according to the parameters of concrete strength, and the volume fraction and the aspect ratio of steel fibers. In order to obtain optimum solutions; equivalent flexural strengths, splitting tensile strength, fracture energy were maximized and cost of fibers were minimized simultaneously. Thus, numerical optimization was used to optimize any combination of either factors or responses.

1 INTRODUCTION

The brittleness of concrete increases with an increase in its strength, i.e. the higher the strength of concrete, the lower is its ductility. Therefore, improving the ductility becomes a major problem for high strength concrete. In concrete, the enhancement of the ductility can be realized by using steel fibers (Balaguru et al.1992, Wafa & Ashour 1992).

Many types of steel fibers are used to reinforce concrete. SFRC is a concrete mix that contains short discrete fibers that are uniformly distributed and randomly oriented. Fibers are originally introduced for the purpose of strengthening the matrix, without distinguishing the difference between the material strength and the material toughness. The addition of steel fibers, especially those with hooked-ends, into concrete significantly improves many of the engineering properties, especially the mechanical and fracture properties, such as impact strength, toughness, resistance to seismic loads, resistance to cracking and ductility. SFRCs are superior to plain concrete because of their higher energy absorption at fracture (Bayramov et al. 2004a).

For a better understanding of the fracture behavior of concrete structures, knowledge of the post-cracking behavior of concrete material is essential. While matrix fails in a brittle manner when it reaches

cracking stresses, the ductile fibers in a fiber-reinforced concrete continue to carry stresses well beyond the matrix cracking, which helps to maintain the structural integrity and cohesiveness of the material (Bayramov et al. 2004a). If properly designed, after matrix cracking, randomly distributed and short fibers arrest microcracks, bridge these cracks, undergo a pullout process and limit crack propagation (Banthia & Trottier 1995, Barros & Figueiras 1999). Debonding and pulling out of the fiber require added energy, giving a substantial increase in toughness and resistance to cyclic and dynamic loading. ASTM C 1018 proposes the evaluation of the toughness indices and JSCE-SF4 recommends using the equivalent flexural strength.

Type, aspect ratio (length/diameter), volume fraction, orientation in the matrix and pull-out resistance of the fibers, as well as matrix properties influence the performance of SFRC (Bayramov et al. 2004b, Bayramov et al. 2004c, Koksall et al. 2006, Yalcin et al. 2007).

The main objective of this work is to determine the performance classes in conventional SFRCs from the equivalent flexural tensile strength point of view. In order to obtain optimum solutions, equivalent flexural tensile strengths for both Serviceability Limit State (SLS) and Ultimate Limit State (ULS), splitting tensile strength and fracture energy were maxi-

mized and the aspect ratio, fiber content and cost of the mixture were minimized simultaneously. For the optimum mix design of SFRCs, three-level factorial experimental design and Response Surface Method were used.

2 EXPERIMENTAL WORK

2.1 Specimen characteristics and production

This experimental work consists of three groups: In the first group, the effect of the same type of hooked end steel fibers on the mechanical and performance properties of concrete having two different concrete classes was investigated. The steel fibers of normal tensile strength have the same aspect ratio ($L/d=80$), but four different volume fractions. Volume fractions of steel fibers were varied between 0.19% and 0.58%, in steps of 0.13%. Thus, in this group, mixtures including two mixtures of control concrete with water-cement ratios of 0.45 and 0.65 and eight mixtures of SFRCs, therefore a total of ten mixtures were produced.

In the second group, the effect of aspect ratio of the steel fiber on the mechanical and performance properties of steel fiber-reinforced concrete was investigated. The normal strength steel fibers having the aspect ratios of 80, 65 and 55 were utilized. In this group, nine concrete series with steel fibers, and one control concrete were cast.

In the third group, the effect of the length and diameter of the fiber on the mechanical and performance properties of concrete was investigated. In this group, the steel fibers of high tensile strength having the same aspect ratio of 80 were used. The lengths of the fibers were 60 mm, 40 mm and 30 mm. In this group, nine concrete series were produced by using high strength steel fibers. Three plain concretes were also prepared as control mixtures. These fibers were added in hybrid form to the mixtures having water-cement ratios of 0.32, 0.44 and 0.75. The steel fibers having the same aspect ratio but different lengths and diameters were used in different amounts. Volume fractions of hybrid steel fibers having high strength were 0.27%, 0.50% and 0.73%. In each hybrid volume fraction, equal volumes from each length were used. Twelve concrete mixtures were produced for this group. Thus, a total of 32 concrete mixtures were produced for this study.

The specimens were cast in steel moulds and compacted on a vibration table. All the specimens were demoulded after about 24 hours, stored under wet burlap at 20°C until 28 days of age, and were then air-cured in the laboratory until their testing date at 56 days. The dimensions of the beams, prepared for four point bending tests, were 150x150x750 mm. At least four beam specimens

from each concrete mixture were tested. For each mixture, three cylinders, 150 mm in diameter and 300 mm in height, were used for compressive strength and modulus of elasticity tests. Six disc specimens, 150 mm in diameter and 60 mm in height, were prepared for the splitting tests.

2.2 Test procedure

Standard strength tests were conducted in accordance with European Standards (EN 206 and EN 12390). Four-point bending tests were performed on the beams of 150x150x750 mm size, as seen in Figure 1a. For the plain concretes, the displacement rate at the mid-span of the beams was kept constant at 0.02 mm/min. The beams with steel fiber, however, were tested at the displacement rate of 0.05 mm/min up to a displacement of 0.5 mm, and then at 0.1 mm/min up to a 5 mm displacement. The load was applied by a Instron 5500R closed-loop testing machine of 100 kN capacity, and displacements were measured simultaneously by using three linear variable displacement transducers (LVDTs). The load versus displacement curve for each beam was obtained by recording the average of three measurements taken at the mid span. The load-displacement curves were used for evaluating the equivalent flexural strengths of both SLS and ULS. As seen in Figure 1b the area under the load versus displacement at mid span curve was described as a measure of the energy required for each displacement.

Characteristic equivalent flexural strength can be calculated as follows:

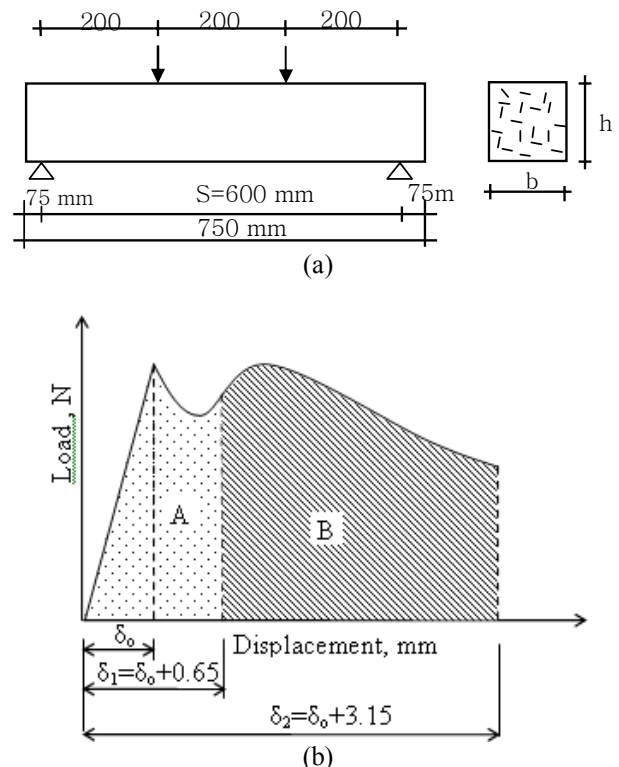


Figure 1. Four point bending test specimen (a), calculation of equivalent tensile strength for each deformation region (b).

$$f_{eq} = \frac{T_i}{\delta_i} \cdot \frac{S}{bh^2} \quad (1)$$

where T_i is the area under load versus displacement curve for serviceability limit state (SLS) or ultimate limit state (ULS), δ_i is the corresponding displacement for each limit state; $b \times h$ (150x150 mm) and S (600 mm) are the cross-section of the beam and the length of the span, respectively.

According to DBV (German Concrete Society), equivalent flexural strengths of steel fiber reinforced concrete are given as indicated in Table 1 (DBV 1996). In this table and in Figure 1, δ_0 shows the displacement at the first crack.

Table 1. Deformation regions for SFRCs.

Deformation Region	Limit State	Displacement
I (small deformation, A)	SLS	$\delta_1 = \delta_0 + 0.65$
II (large deformation, A+B)	ULS	$\delta_2 = \delta_0 + 3.15$

3 RESULTS AND DISCUSSION

3.1 Compressive behavior of SFRCs

In the first group, a decrease in the water-cement ratio from 0.65 to 0.45 has resulted in an increase of 55% in the compressive strength of concrete without steel fiber. The effect of fiber volume fraction on compressive strength of SFRC is not consistent for each concrete class. For each water/cement ratio, there is also no significant effect of fiber volume fraction on the modulus of elasticity. According to the second group of test results, similar to the first group, there is no significant change in compressive strength or modulus of elasticity, when the plain and steel fiber reinforced concretes are compared.

In concrete with hybrid high strength steel fibers, for each water/cement ratio, effect of fiber volume fraction on both compressive strength and modulus of elasticity is not significant. However, the addition of steel fibers into concrete has an effect of increasing the ductility in the compressive failure rather than the compressive strength.

For the stress-strain curve of concrete with and without fibers, cylinder specimens were tested under compression using an Instron closed-loop testing machine with a capacity of 5000 kN. The longitudinal displacement was controlled by an LVDT placed on a specially designed frame alongside the test specimen which monitored the axial deformation of the specimen. This LVDT was also used as the feed back signal. Another LVDT was also placed on the frame mentioned. The data from two LVDTs and load were recorded simultaneously.

A typical stress-strain curve of concretes with the same water/cement ratio of 0.44 is shown in Figure 2. As seen in this figure, compressive strengths of concretes with hybrid fibers are very close to each other and the relative absorbed fracture energies up to the peak stresses are almost identical. However, as seen in the figure when the volume fraction of fibers increases, after the peak stress more energy is dissipated and material becomes more ductile. In other words, the total fracture energy of concrete with low content of steel fiber decreases significantly in concrete.

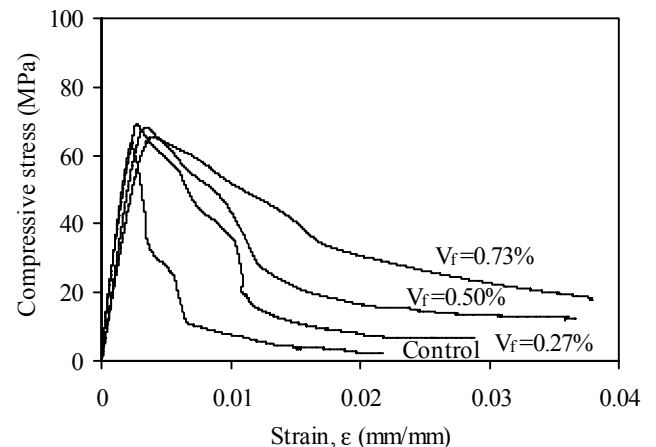


Figure 2. Typical compressive stress-strain curves of concretes with high strength hybrid steel fibers ($w/c=0.44$, $L/d=80$).

For the three different water/cement ratios, typical stress-strain curves of concretes with the same volume fraction of hybrid fibers ($V_f=0.73\%$) are shown in Figure 3. As seen in this figure, for the concrete with water/cement ratio of 0.32, the curve of the concrete having high compressive strength is almost linear up to the peak stress, and there is a sudden drop of stress at the beginning of post-peak response.

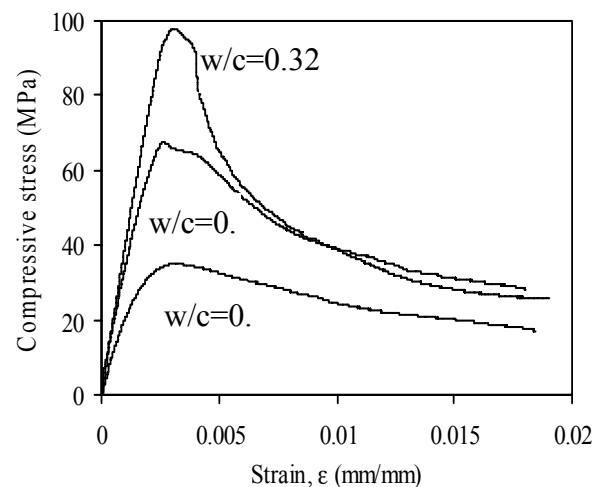


Figure 3. Effect of water/cement ratio on the compressive stress-strain curve of concrete under compression ($V_f=0.73\%$).

3.2 Splitting tensile strength

In the first group of the tests, it was seen that the increase in steel fiber volume fraction from 0 (i.e. normal concrete) to 0.58% has resulted in an increase of 26% in corresponding splitting tensile strength. For the water/cement ratio of 0.65, however, this increase was only 10%. Thus, it can be concluded that more significant results were obtained in SFRC mixtures with low water/cement ratios such as 0.45.

In second group, it is shown that the splitting tensile strength increases slowly with increasing steel fiber volume fraction (V_f) for all the aspect ratios of 80, 65 and 55. The highest increase compared to plain concrete could be obtained with the usage of steel fibers that have the aspect ratio of 80. For the specific splitting tensile strength value of 4.51 MPa, fibers with the aspect ratio of 55 should be used at 0.51% (40 kg/m^3), while the fibers with the aspect ratio of 80 could be used at 0.38% (30 kg/m^3).

In the third group of experiments, there is significant increase in the splitting tensile strengths of SFRCs with the increase in volume fractions of high strength steel fibers at the lower water/cement ratio such as 0.32 and 0.44, however, in SFRCs with high values of water/cement ratio (0.75), there is a slight increase with respect to volume fraction of the fibers. Details of these test results can be found in Yalcin (2009).

3.3 Flexural strengths

In the first group, flexural strength (f_{flex}) increases as the fiber volume fraction increases; the increase in the fiber volume fraction from 0 (i.e. normal concrete) to 0.58%, has resulted in an increase of 46%, for the water/cement ratio of 0.45, the increase was 70%. In the second and third groups, depending on the aspect ratio and the fiber volume fraction, significant increases in flexural strength were recorded.

Fracture process of SFRC consists of progressive debonding of fibers, during which slow crack propagation occurs. Final failure occurs due to unstable crack propagation when the fibers are pulled out and the interfacial shear stress reaches the ultimate strength. The reason for the increase in flexural strength is that, after matrix cracking, fibers carry the load subjected to concrete until the cracking of interfacial bond between fibers and matrix occurs (Gao et al. 1999)

As seen in Figure 4, flexural strength of SFRCs can be expressed in terms of the variable $V_f(L/d)$ as follows:

$$f_{flex} = f_m + C_1 V_f (L/d) + C_2 \left[V_f (L/d) \right]^2 \quad (2)$$

where f_m is the flexural strength of plain concrete

(i.e. matrix), and C_1 and C_2 are coefficients which were determined by experiments. In the relation shown by Equation 2, the correlation is high (0.93) and the equation is valid for a range of concretes prepared in this work.

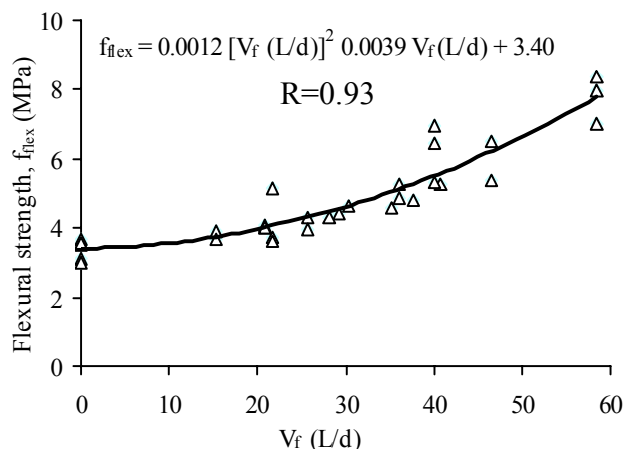


Figure 4. Flexural strength versus the variable $V_f(L/d)$.

3.4 Complete load-displacement curves under bending

Based on the second group of experiments, typical load-displacement curves for the mixture containing fibers with the aspect ratio of 80 are shown in Figure 5. These curves obtained in this study were used for evaluating the equivalent flexural strengths for both SLS and ULS. The area under each curve was indicated to be a measure of the fracture energy of the material. It can clearly be seen that fracture energy increases as the fiber volume fraction of steel fiber increases. As seen in the figure, after the formation of the first crack, except the mixture with the steel fiber volume fraction of 0.32%, the progress of strain hardening in the ascending branch of the curve is a typical indication of high performance cement based composites. Similar results were obtained for the mixtures with the other aspect ratios.

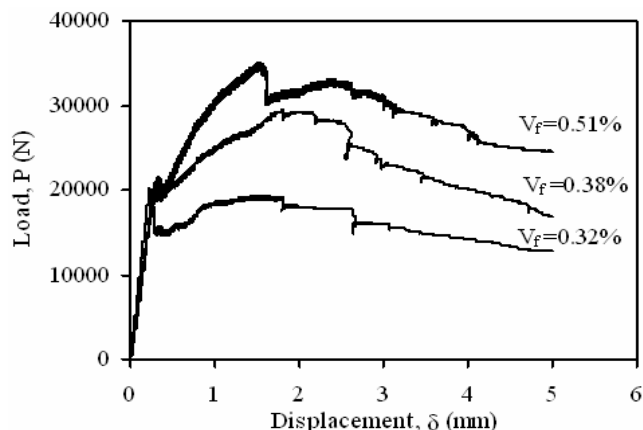


Figure 5. Typical load versus displacement at the midspan-curves for the second group of mixtures containing fibers with the aspect ratio of 80.

3.5 Fracture energy

For the three groups of experiments, it is shown that the ability of the beam to absorb energy is substantial, even though the cut-off point was taken at the specified displacement of 5mm. Experimental results obtained show that SFRCs allow high values of fracture energies as a result of their high ductility depending on their matrices, aspect ratios and the contents of fibers used. The increase in the fracture energy is because of the fiber fracture pull-out and fiber debonding in the fracture process. Great number of fibers form a bridge along crack and therefore more tortuous crack propagation is obtained (Bayramov et al. 2004c).

Fracture energy can be represented by using the variable $V_f(L/d)$ as follows

$$G_f = G_m + k_1 V_f(L/d) + k_2 \left[V_f(L/d) \right]^2 \quad (3)$$

where G_m is the fracture energy of plain concrete (i.e. matrix), k_1 and k_2 are coefficients which are determined by the experiments.

The variable $V_f(L/d)$ is a very useful tool representing fracture energy; the function above was fitted to the experimental data and a good correlation coefficient of 0.95 was found for a range of fracture energies between 176 J/m² (plain concrete) and 8000 J/m². As shown in Figure 6, fracture energies were calculated from bending test tests of all three groups.

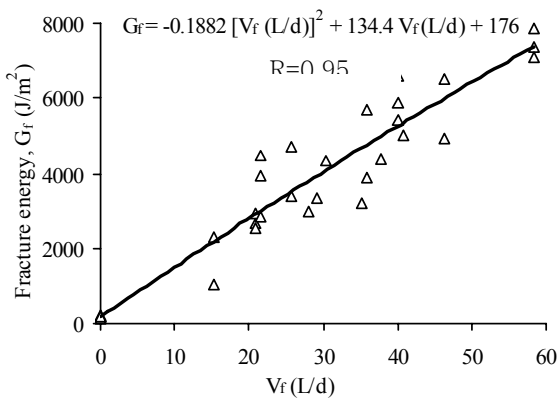


Figure 6. Fracture energy versus the variable $V_f(L/d)$.

3.6 Equivalent flexural strengths for serviceability and ultimate limit states

One of the major roles of fibers in concrete is to provide an increase in the fracture energy. The results obtained were based on the area under the complete load-displacement curve up to a specified displacement. The specified displacements for SLS and ULS are $\delta_0 + 0.65$ mm and $\delta_0 + 3.15$ mm, respectively. In Figure 5, the cut-off point was chosen as 5 mm displacement. It is seen in the curves in the figure that, the energy at this displacement (i.e 5mm), however is

not totally dissipated. As seen in Figure 7, SFRCs provide high values of equivalent flexural strengths as a result of a high ductility; depending on the aspect ratios and volume fractions of fibers used. The increase in equivalent strengths for both SLS and ULS is because of the high energy absorbed due to fiber pull-out and fiber debonding in the fracture process.

Figure 7 shows the effects of aspect ratio and fiber content on the equivalent stresses for SLS and ULS. For a certain volume fraction of hooked end steel fibers, the equivalent strengths (f_{eq-I} , f_{eq-II}) increase significantly, as the aspect ratio of SFRC increases. In SFRCs with the aspect ratio of 80, f_{eq-II} increases rapidly with the increasing steel fiber volume fraction. It should be noted that these experimental results are valid for normal strength matrix and low carbon steel fiber; which has a yield strength of 1100 MPa. It can be concluded that the capability of the beam to absorb energy is substantial, even if the cut-off point is taken at the specified displacements of $\delta_0 + 0.65$ and $\delta_0 + 3.15$ mm. Figures 7a and 7b show the effects of fiber content on the equivalent flexural tensile strengths for both SLS and ULS for three different aspect ratios. As seen in these figures, for a certain volume fraction of hooked end steel fibers, equivalent flexural tensile strength (f_{eq-I} or f_{eq-II}) increases significantly as the aspect ratio of steel fiber increases. For a certain concrete class it is seen that, the fiber content and aspect ratio are the main variables in determining the performance classes of SFRCs (Bayramov et al. 2002, Falker et al. 1999). Hence, it can be concluded that the results obtained give a clear picture of how a quasi-brittle concrete transforms into a ductile composite with the addition of steel fibers.

Based on the test results obtained in this work, the performance classes of SFRCs for both small and large deformations (i.e. SLS and ULS) can be given. For example, the performance class of SFRC with water/cement ratio of 0.55, fiber volume fraction of 0.51% and aspect ratio of 80 can be denoted by C35/45 F 3.54/4.21. Similarly, the performance class of the mixture ($L/d=65$ and $V_f=0.45\%$) can be said to be C35/45 F 3.11/2.82.

4 OPTIMIZATION

In this study, for the second group of experiments a multi-objective simultaneous optimization technique was used in which Response Surface Method (RSM) is incorporated. For this purpose, in the second group, nine experimental data for each response of SFRCs, were fitted to the mathematical model by using analysis of variance (ANOVA). For each mechanical property of SFRCs in each series, the fitted

regression models for fracture energy are given below:

$$G_f = 2.13 - 0.10 V_f - 0.017 L/d + 0.0027 (V_f)(L/d)$$

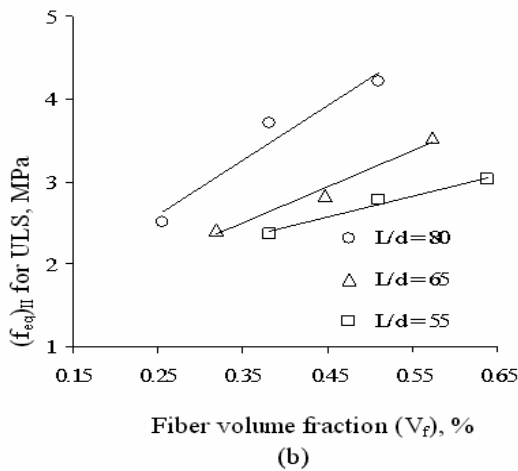
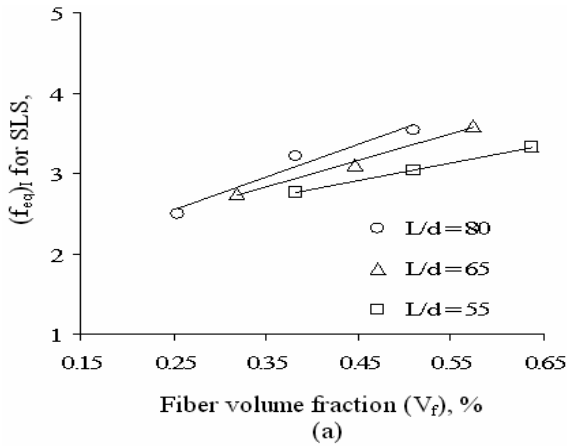


Figure 7. Equivalent flexural strength versus fiber volume fraction curves for SLS (a), equivalent flexural strength versus fiber volume fraction curves for ULS (b) (Group 2, w/c=0.55).

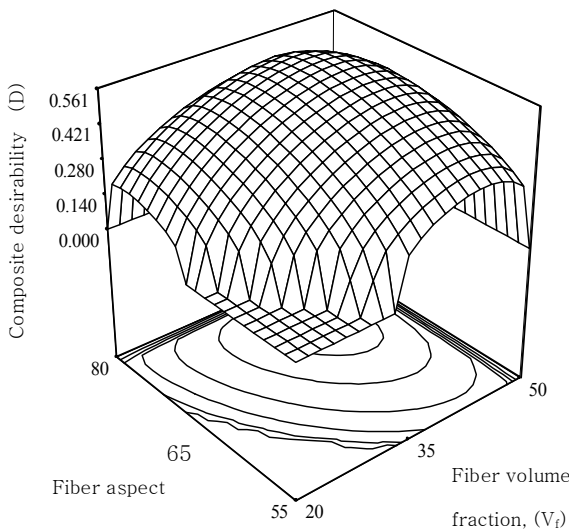


Figure 8. Response surface plot of the composite desirability (D) when f_{eq-I} , f_{eq-II} , f_{sp} and G_f are maximized and fiber content (V_c), L/d and cost of mixture are minimized simultaneously (Group 2).

Solving such multiple response optimization problems using desirability technique involves using a technique for combining multiple responses into a dimensionless measure of performance called the overall desirability function (Derringer & Suich 1980). The desirability approach involves transforming each estimated response, d_i , into a unitless utility bounded by $0 < d_i < 1$.

In case of maximizing and minimizing of individual responses, the desirability will be defined by the formulas given in Equations 4 and 5, respectively.

$$d_i = \begin{cases} 0 & Y_i \leq \min f_i \\ \left(\frac{Y_i - \min f_i}{\max f_i - \min f_i} \right)^{wt} & \min f_i < Y_i < \max f_i \\ 1 & Y_i \geq \max f_i \end{cases} \quad (4)$$

$$d_i = \begin{cases} 1 & Y_i \leq \min f_i \\ \left(\frac{\max f_i - Y_i}{\max f_i - \min f_i} \right)^{wt} & \min f_i < Y_i < \max f_i \\ 0 & Y_i \geq \max f_i \end{cases} \quad (5)$$

A multi-objective optimization problem is solved by using the single composite response (D) given in Equation 6, which is the geometric mean of the individual desirability function (Myers & Montgomery 1995).

$$D = (d_1 \times d_2 \times \dots \times d_n)^{\frac{1}{n}} = \left(\prod_{i=1}^n d_i \right)^{\frac{1}{n}} \quad (6)$$

where n is the number of response included in the optimization.

After building the regression models, all independent variables are varied simultaneously and independently in order to optimize the objective func-

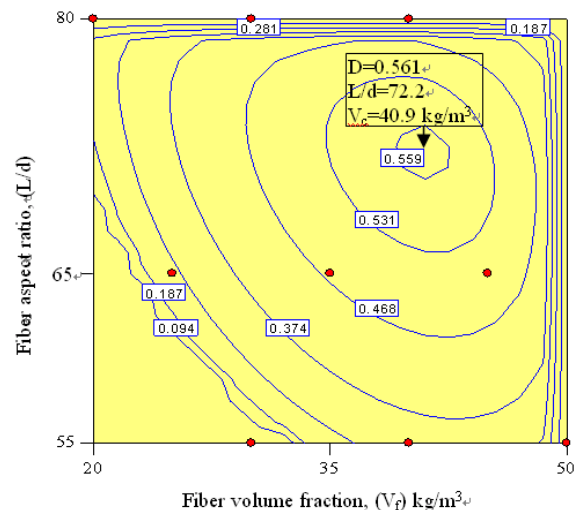


Figure 9. Contour plot of composite desirability (D) when f_{eq-I} , f_{eq-II} , f_{sp} , f_{sp} and G_f are maximized and V_c , L/d and cost of mixture are minimized simultaneously (Group 2).

Table 2. Performance classes for SFRCs.

W/C	Concrete class	Fiber type	Fiber volume fraction V_f , %	Equivalent flexural strengths, MPa		Performance classes
				f_{eq-I} (SLS)	f_{eq-II} (ULS)	
0.45	C40/50		0.19	2.39	2.00	C40/50 NSF 2.39/2.00
			0.32	3.48	3.67	C40/50 NSF 3.48/3.67
			0.45	3.86	4.16	C40/50 NSF 3.86/4.16
			NS	4.18	5.26	C40/50 NSF 4.18/5.26
0.65	C30/37	80/60	0.19	2.08	1.53	C30/37 NSF 2.08/1.53
			0.32	2.38	2.75	C30/37 NSF 2.38/2.75
		0.45	2.94	3.53	C30/37 NSF 2.94/3.53	
		0.58	3.38	4.60	C30/37 NSF 3.38/4.60	
		NS	2.49	2.51	C35/45 NSF 2.49/2.51	
		80/60	0.38	3.22	3.70	C35/45 NSF 3.22/3.70
0.55	C35/45	NS	0.51	3.54	4.21	C35/45 NSF 3.54/4.21
			0.32	2.75	2.42	C35/45 NSF 2.75/2.42
		65/60	0.45	3.11	2.82	C35/45 NSF 3.11/2.82
			0.58	3.60	3.53	C35/45 NSF 3.60/3.53
		NS	0.38	2.76	2.37	C35/45 NSF 2.76/2.37
			55/60	0.51	3.03	2.78
0.32	C80/95		0.64	3.32	3.02	C35/45 NSF 3.32/3.02
			0.27	3.04	4.37	C80/95 HSF 3.04/4.37
			0.50	3.62	5.26	C80/95 HSF 3.62/5.26
			0.73	4.39	6.13	C80/95 HSF 4.39/6.13
0.44	C55/67	HS	0.27	2.37	2.90	C55/67 HSF 2.37/2.90
			0.50	3.37	5.08	C55/67 HSF 3.37/5.08
			0.73	3.96	6.26	C55/67 HSF 3.96/6.26
			0.27	2.19	2.23	C25/30 HSF 2.19/2.23
0.75	C25/30		0.50	3.19	4.35	C25/30 HSF 3.19/4.35
			0.73	3.69	5.49	C25/30 HSF 3.69/5.49

tions. For the second group of this work, composite desirability (D) for this multi objective optimization is shown in Figures 8 and 9. Here the optimal values of design variables are $L/d=72.2$, $V_c=40.9 \text{ kg/m}^3$, and cost of mixture is 1.97 unit.

5 PERFORMANCE CLASSES FOR SFRCs

Based on the three groups of experiments and within the limits of this work, performance classes of SFRC can be determined according to both SLS and ULS. The results obtained are shown in Table 2. In case of high volume fractions and high aspect ratios of steel fibers as in groups 1 and 2 and also in all concretes with hybrid high strength steel fibers, the values of equivalent flexural strength determined according to ULS are higher than those of SLSs. The Reason for this is that, after the formation of the first crack, a typical strain hardening behavior is observed in these mixtures except the mixtures with low volume fractions and low aspect ratios, and also low strength of plain concrete.

6 CONCLUSIONS

Based on the experimental test results obtained and evaluated in this work, the following conclusions can be drawn:

1) For a certain aspect ratio, as the steel fiber volume fraction increases, mixtures with lower water cement ratio give higher equivalent flexural strengths for both serviceability and ultimate limit states.

2) After the formation of the first crack, in all mixtures except the mixtures with the low value of steel fiber volume fractions and aspect ratios, the typical strain hardening in the ascending branch of the load-displacement curve is an indication of high performance cementitious composites.

3) For a certain concrete class, the equivalent flexural tensile strengths depend on both the fiber volume fraction and the fiber aspect ratio. The mixture with the longer steel fibers provides higher equivalent flexural tensile strength values than those of shorter ones.

4) Within the limits of this work, in mixtures having a certain water-cement ratio, there is no significant effect of fiber volume fraction on the compressive strength or the modulus of elasticity. In concretes with hybrid high strength steel fibers, for a certain water/cement ratio the addition of steel fibers into concrete has an effect of increasing the ductility in compressive failure rather than the compressive strength.

5) Response surface method (RSM) is a promising approach for optimizing steel fiber reinforced concrete (SFRCs) to meet several performance criteria such as minimum cost and brittleness. The experimental design made by using RSM provides a

thorough examination of SFRC properties over the selected range of fiber volume fraction and aspect ratio, and the strength of concrete. In order to provide an adequate representation of the responses, fitting mathematical models that are usually assumed to represent each concrete property of interest, can be done in identifying optimal mixtures. The results show that the predictiveness of the regression model is satisfactory.

6) Performance classification of SFRCs can be made according to the parameters of concrete strength class and the volume fraction and aspect ratio of steel fibers. The cost of the steel fiber used in the production of SFRCs is also important from the application point of view. The volume fraction and aspect ratio of steel fiber must be minimized, however, in order to get an optimal mixture, the equivalent flexural tensile strength, splitting tensile strength and fracture energy should be maximized. Thus, numerical optimization can be used to optimize any combination of either factors or responses. The cost of steel fibers with the high aspect ratio is higher than that of the lower ones, but their performances are in contrary to their prices. Since the designer is interested in the equivalent flexural tensile strength, but not in the price of steel fibers, SFRC producer should find an optimum solution. In the future, it is expected that, in the determination of the performance classes of SFRCs, in addition to the concrete strength, the properties such as ductility and durability in the hardened state and workability in fresh state will also be considered.

7 ACKNOWLEDGEMENT

This research was completed in the Faculty of Civil Engineering at Istanbul Technical University (ITU). The concrete production part of this study was done at Akansa Betonsa Technological Center. The third author wish to acknowledge Scientific and Technological Research Council of Turkey (Project: 106G122, Kamu). The support given by BEKAERT is also gratefully acknowledged.

REFERENCES

Balaguru P., Narahari, R. & Patel, M. 1992. Flexural toughness of steel fibre reinforced concrete, *ACI Mater. J.* 89(6):541-546.

Banthia, N. & Trotter, J.F. 1995. Concrete reinforced with deformed steel fibres, Part II: Toughness characterization, *ACI Material Journal* 92(2): 146-154.

Barros, J.A.O & Figueiras, J.A. 1999. Flexural behaviour of SFRC: testing and modeling, *J. Mater. Civ. Eng.* 11(4): 331-339.

Bayramov, F., Tasdemir, C. & Tasdemir, M. A. 2002. Optimum Design of Cement-Based Composite Materials using Statistical Response Surface Method, *ACE 2002: Fifth In-*

ternational Congress on Advances in Civil Engineering, 25-27 September, (2): 725-734. Istanbul, Turkey

Bayramov, F., Ilki, A., Tasdemir, M.A. & Yerlikaya, M. 2004a. SFRCs for Concrete Roads in Heavily Trafficked Situations,. 9th. International Symposium on Concrete Roads, 4-7 April, Istanbul.

Bayramov, F., Ilki, A., Tasdemir, C. & Tasdemir, M.A. 2004b. An optimum design of steel fiber reinforced concretes under cyclic loading. In: *Proc. FraMCoS-5*, April 12-16, (2): 1121-1128, Vail, Colorado.

Bayramov, F., Tasdemir, C. & Tasdemir, M.A. 2004c. Optimisation of steel fiber reinforced concrete by means of statistical response surface method, *Cement and Concrete Composites*, (26): 665-675.

DBV, Recommendation: 1996. Basis for the design of industrial floor slabs out of steel fiber reinforced concrete. Eigenverlag, Wiesbaden.

Derringer, G. & Suich, R. 1980. Simultaneous optimization of several response variables, *Journal of Quality Technology*, 12(4): 214-219.

Falkner, H., Teutsch, N. & Klinkert, H. 1999. Leistungsklassen von stablfaserbeton, Institut für Baustoffe, Massivbau und Brandschutz, TU Braunschweig, 36 pp.

Gao, J., Sun, W. & Morino, K. 1999. Mechanical properties of steel fiber reinforced, high strength, and lightweight concrete, *Cement and Concrete Composites*, (19): 307-313.

Koksal, F., Ilki, A., Bayramov, F. & Tasdemir, M.A. 2006. Mechanical behaviour and optimum design of SFRC plates, *16th European Conference of Fracture, MMMCP, S.P. Shah Symposium*, July 3-7, Springer Verlag, 199-205, Alexandroupolis, Greece.

Myers R.H. & Montgomery, D.C. 1995. Response Surface Methodology: Process And Product Optimization Using Designed Experiment, John Wiley & Sons, New York.

Wafa, F.F. & Ashour, S.A., 1992, Mechanical properties of high-strength fibre reinforced concrete, *ACI Mater. J.* 89(5):449-455.

Yalcin, M., Sengul, C., Tasdemir, C., Gokalp, I., Yuceer, Z. & Ekim, H. 2007. Performance based design of steel fiber reinforced concrete, *TCMA 3rd International Symposium, Sustainability in Cement and Concrete*, 931- 940, Istanbul, Turkey.

Yalcin, M. 2009. Optimization and Performance Based Design of Steel Fiber Reinforced Concretes, PhD Thesis, Istanbul Technical University, Institute of Science and Technology, 205p.